

Available online at [www.sciencedirect.com](http://www.sciencedirect.com)

ScienceDirect

journal homepage: <http://www.elsevier.com/locate/acme>

## Original Research Article

# Structure and properties of AlMg alloy after combination of ECAP and post-ECAP ageing

T. Tański<sup>a,\*</sup>, P. Snopiński<sup>a</sup>, W. Pakieła<sup>a</sup>, W. Borek<sup>a</sup>, K. Prusik<sup>b</sup>, S. Rusz<sup>c</sup>

<sup>a</sup> Division of Material Processing Technology, Management and Computer Techniques in Materials Science, Institute of Engineering Materials and Biomaterials, Silesian University of Technology, ul. Konarskiego 18a, 44-100 Gliwice, Poland

<sup>b</sup> Faculty of Computer Science and Materials Science, University of Silesia, ul. 75 Pułku Piechoty 1A, 41-500 Chorzów, Poland

<sup>c</sup> VŠB-Technical University of Ostrava, 17. listopadu 15, 708 33 Ostrava, Czech Republic

## ARTICLE INFO

## Article history:

Received 2 January 2015

Accepted 20 December 2015

Available online 27 February 2016

## Keywords:

Severe plastic deformation

ECAP

Aluminium alloy

Structure

Tensile properties

## ABSTRACT

Equal channel angular pressing technique (ECAP) was used before and after solution heat treatment to obtain grain refinement and strengthening of commercial Al–Mg casting alloys. The experiments were performed to investigate the strengthening effect of the alloy after various post-ECAP ageing treatments. The alloys were severely deformed at room temperature following route B<sub>c</sub> and die channel angle of 120°. It was found that heat treatment before and after ECAP significantly affect and improves mechanical properties of aluminium alloys. It was also proven that the severe plastic deformation causes grain refinement which directly influence on properties of AlMg alloys. An increase of strength and ductility was achieved by appropriate selection of post-ECAP ageing. It is also proven that the good strengthening effect is also achieved at temperatures lower than those usually used for ageing. Based on the findings above, the tensile properties and hardness of Al–Mg alloys are discussed.

© 2015 Politechnika Wroclawska. Published by Elsevier Sp. z o.o. All rights reserved.

## 1. Introduction

Since many years it is known that large accumulation of plastic strain has a significant impact on the microstructure and mechanical properties of materials. As an example one can use the well-known processes of drawing or cold rolling, which are accompanied by intensive grain refinement, that results in an increase of material properties [1]. However, conventional methods of plastic working, very often result in

ductility decrease, which in many applications is undesirable and sometimes unacceptable [2,3]. These restrictions resulted in an increased interest in the development of new methods of severe plastic deformation (SPD) [4], allowing manufacturing of materials which have finely refined microstructures and exhibits a completely new physical and mechanical properties, including increased plasticity [5–7]. Metal forming using severe plastic deformation becomes more commonly used, due to the possibility of achieving a large grain refinement from sub-micrometre to nanometer size in metallic materials.

\* Corresponding author.

E-mail address: [tomasz.tanski@polsl.pl](mailto:tomasz.tanski@polsl.pl) (T. Tański).

<http://dx.doi.org/10.1016/j.acme.2015.12.004>

1644-9665/© 2015 Politechnika Wroclawska. Published by Elsevier Sp. z o.o. All rights reserved.

**Table 1 – Chemical composition of grade ENAC-AlMg3 (ENAC-51100).**

Fe	Si	Mn	Ti	Cu	Mg	Zn	Al
Max. 0.55	Max. 0.55	Max. 0.45	Max. 0.2	Max. 0.05	2.5–3.5	Max. 0.1	Rest

There are many methods of SPD, but the most common technique, which focuses the highest attention of scientist in recent years has become the ECAP method [8].

Equal channel angular pressing is metal forming procedure, allowing an introduction very large amounts of strain into a metal or alloy [9]. As a work-specimen is pressed through a die, it is constrained to deform primarily by simple shear along the plane of intersection between two channels (having an interior angle of 120° in the current study). Due to the fact that both channels are equal in cross-sections, the work sample may be placed back on the input of the channel for subsequent deformation [10,11]. In addition there is also possibility to rotate specimen between each passes in order to change the inclination of the shear bands in the metal structure. In this way, various microstructures and crystallographic textures may be produced. A nomenclature has been adopted in the literature denoting the possible routes A, B<sub>a</sub>, B<sub>c</sub>, and C. Through years a lot of work was devoted in order to examine possibility of fabrication previously unobserved structures and properties in large variety of metals and it's alloys, especially to obtain an increase in mechanical properties of light metals like aluminium or magnesium through grain refinement or changing of crystallographic textures [12].

However at present scientists have expressed greater interest in not only the traditional heat treatment or intensive plastic deformation trying to investigate the effect of combination heat and plastic treatment on the properties of many metals including steel or light alloys [13,14]. Hence, it becomes necessary to accurately understand the mechanism that cause synergism strengthening in aluminium magnesium alloys using low-temperature annealing which is known as the post-ECAP ageing that in many cases results in a further increase in mechanical properties or increase ductility without significant decrease in material properties [15,16].

The present investigation was initiated in order to determine an influence of solid solution treatment before ECAP process and post ECAP ageing on structure and properties of aluminium alloy [17,18]. First stage of investigation was feasibility of achieving significant grain refinement of AlMg3 alloy at room temperature, and after ageing. The second examination was to determine tensile properties of these pressed materials and determination of the best type of thermo-mechanical treatment of presented aluminium alloy [14,19].

## 2. Experimental procedure

### 2.1. Material

The investigation was carried out on casting aluminium alloy ENAC-AlMg3 – 51100. Because of its very good properties such as good corrosion resistant because of increased Mg content

found a wide range of applications. Another advantage of this alloy is possibility to perform the heat treatment, which permits obtaining increased mechanical properties. The chemical composition of investigated material is shown in Table 1.

### 2.2. Heat treatment and ECAP process

First stage of experiment was to find a most beneficial heat treatment conditions, therefore material was subjected to solution treatment at 580 °C (below solidus temperature) and then artificially aged at 160 °C for 4, 8 and 12 h. Second stage was Equal channel angular pressing that was carried out using a die with an internal angle ( $\phi$ ) of 120°. As a lubricant was used molybdenum sulfide (MoS<sub>2</sub>). Rods with diameter of 20 mm and length of 80 mm were pre-machined from as cast material. Solution treatment was conducted at 580 °C for 8 h and then specimens were quenched in room temperature water. Then were pressed through the ECAP die at room temperature. Four repetitive pressing were carried out on each sample with rotation about longitudinal axis by 90° in the same direction, this procedure has been designated as route B<sub>c</sub>. After ECAP process those specimens were aged at 160 °C and 100 °C for 2 and 4 h in order to get the higher hardness according to precipitation hardening. To verify ageing potential of as cast material, without solution heat treatment, static ageing was also conducted at the same temperature and time on specimens without solution treatment.

### 2.3. Investigations procedure

Metallographic samples were taken from a location in the middle of the sample. In order to determine grain contrast as polished samples were anodized using Barker's reagent (5 ml HBF<sub>4</sub> 48% in 200 ml H<sub>2</sub>O, 20 V). The microstructure of the alloy before and after ECAP were characterized using light optical microscope Axio Observer Image Analyser and observed under polarized light, and using C-DIC contrast on cross sections of the specimens. Chemical composition microanalysis was prepared on the scanning electron microscope ZEISS Supra using Energy-dispersive X-ray spectroscopy. Grain size measurement was performed using line intersection method. The examinations of thin foils microstructure and phase identification were made on the high resolution transmission electron microscope JEM 3010UHR from JEOL, at the accelerating voltage of 300 kV. TEM specimens were prepared by cutting thin plates from the material. The specimens were ground down to foils with a maximum thickness of 80 μm before 3 mm diameter discs were punched from the specimens. The disks were further thinned by ion milling method with the Precision Ion Polishing System (PIPS™), used the ion milling device model 691 supplied by Gatan until one or more holes appeared. The ion milling was done with argon ions, accelerated by a voltage of 15 kV.

Static tensile test and microhardness were performed to compare strength and ductility of as pressed material to initial state. Vickers microhardness ( $H_V$ ) was measured on cross-section plain designated as  $\gamma$ -plane by imposing a load of 300 g for 15 s using Vickers hardness tester Future-Tech FM-ARS. All of the tensile tests in current investigation were performed at room temperature using a universal tensile testing machine ZWICK Z/100. The tribological test was performed using CMS Instruments tribometer. Investigations were made in dry friction conditions. Wear resistance test was performed on a distance 50 m and section 5 mm under load 10 N. As the back specimen the  $Al_2O_3$  ball was used.

X-ray diffraction analysis were carried out on PANalytical X'Pert Pro diffraction system with cobalt anode ( $K_{\alpha} = 1.789 \text{ \AA}$ ) in order to determine the average lattice strain. Stress measurements were performed on cross-sectional axis using  $\sin^2 \psi$  technique basing on the Stress X'Pert Plus software. Samples for XRD measurements were well polished and the investigation was conducted on cross sections of specimens and repeated two times for each sample.

### 3. Investigation results

#### 3.1. Microstructure and grain size

The initial state (as cast) structure of investigated alloy taken in SEM microscope is shown in Fig. 1 and the results of pointwise chemical composition analysis are listed in Table 2. In accordance to the binary Al-Mg phase diagram structure of AlMg3 alloy consist of two phases:  $\alpha$ -Al which is a matrix and  $\beta$ - $Al_3Mg_2$ . The presence of  $\beta$ - $Al_3Mg_2$  phase in Al-Mg alloys was confirmed by Stranik et al. [20]. However the chemical composition given in Table 2 indicates that there is possibility of forming other precipitates. The results of EDS analysis confirms that thesis because there are also some precipitates containing Si which are probably  $Mg_2Si$ . To characterize grain size change in investigated material, polarized light structures were taken (Fig. 2a–c). As it could be seen an initial state alloy has relatively large grain size approx.  $331 \mu\text{m}$  (Table 3) and the dendritic segregation in structure is clearly seen. It should be also noticed that individual grains are separated by low angle boundaries. Solution treatment provides to obtaining more uniform structure. There are few precipitates located near the grain boundaries, which puts forward a proposal that

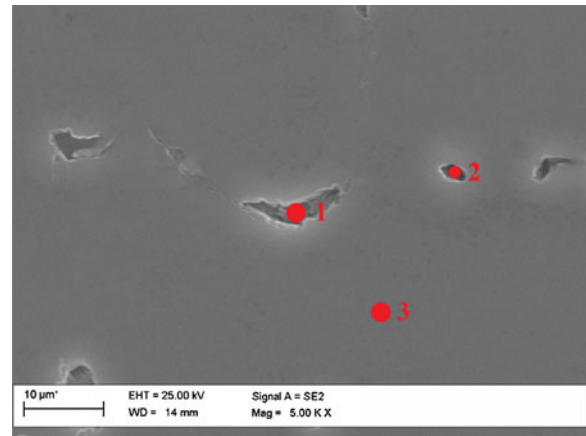


Fig. 1 – Initial state microstructure of investigated alloy.

$\beta$ - $Al_3Mg_2$  phase dissolve in matrix (Fig. 2b). The grain size in alloy after solution treatment is lower which also is shown on the histograms of grain size distribution placed in (Fig. 4a–c). Smaller grain size of solution treated material may be explained by higher cooling rate of heat treated alloy. It can be seen that after solutionizing volume fraction of grains in the range of 100 to  $300 \mu\text{m}$  increases comparing to initial state alloy which is directly confirmed by the measurement of grain size. An average grain size after solution treatment is  $294 \mu\text{m}$ . Fig. 2c illustrates the evolution of microstructure an alloy subjected to ECAP process after solution treatment. As it could be observed grains are still relatively large and are inclined by shearing bands. An average grain size after four passes of ECAP process is  $263 \mu\text{m}$ . It is apparent that the microstructure is refined by the interaction of shear bands, slip bands (Fig. 3a and b) and their increase in number which result in smaller subgrain size Rusz et al. [21]. The grains looks highly deformed which correspond to the route  $B_c$  that provides largest grain refinement and the most uniform structure which was also confirmed by Valiev et al. [9]. The ageing process after ECAP do not provide to any changes in grain size that could be observed using standard metallographic techniques because the early stages of recrystallization process proceed on the subgrain level which do not allow observing that changes using light microscopy which also confirms Wang et al. [15]. Fig. 5a and b represents the microstructure of investigated alloy subjected

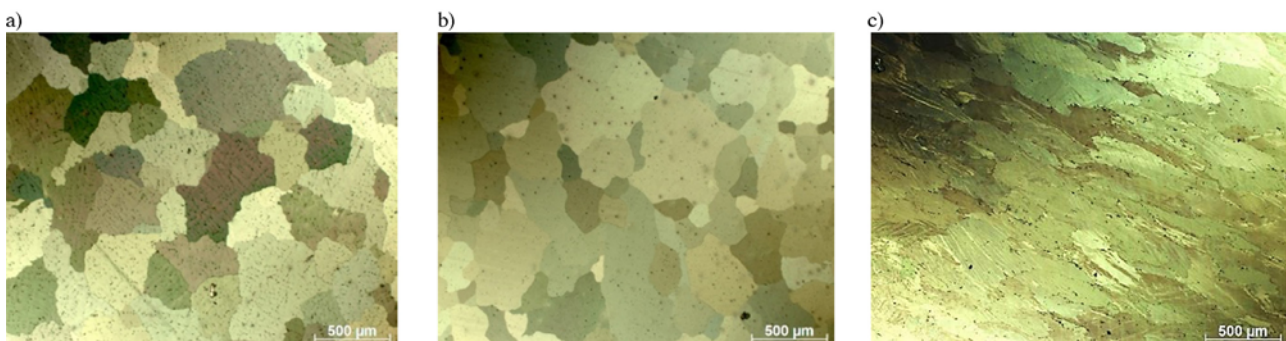


Fig. 2 – Polarized light images of AlMg3 alloy (a) initial state, (b) solution treated, (c) solution treated and ECAPed 4× (processing route  $B_c$ ).

**Table 2 – Pointwise chemical composition analysis from Fig. 2.**

Point	Element	Wt%	At%
1	MgK	22.75	24.63
	AlK	77.25	75.37
2	MgK	17.98	19.60
	AlK	77.10	75.75
	SiK	04.92	04.64
3	MgK	03.90	04.32
	AlK	96.10	95.68

**Table 3 – Results of grain size measurement.**

Condition	Initial state	Solution treated	Solution treated and ECAPed 4× route B <sub>c</sub>
Grain size (μm)	331	294	263

to ECAP process before and after ageing correspondingly. It is clearly visible that after solution treatment there are some β phase precipitates on the grain boundaries. Further ageing of ECAPed material (Fig. 5b) provides to obtaining more uniform distribution of β (red marked precipitates) phases that precipitate from supersaturated solid solution. The precipitation sequence in the AlMg alloy was well characterized by Starink et al. [20].

The TEM structure analysis confirms the thesis stated above. Fig. 6a–d presents the substructure of the AlMg3 alloy subjected to artificial ageing in 2 h after severe plastic deformation. Observation was prepared on the cross-section of as deformed samples. It can be observed that the individual grains of size ~200 nm became elongated in one of the direction. The reason of this effect are shearing forces affecting sample during deformation. Fig. 7a shows representative TEM image illustrating high dislocation density area. Comparison with Fig. 6a or c it may be stated that in heat treatment affected sample, are present dislocation free areas and those with high density of defects. Fig. 7b shows a diffraction pattern from the area presented in Fig. 7a. Solution of this diffraction presented in Fig. 7c confirms conclusion that dominant phase is α-Al. However, as it was previously assumed, substructure of investigated alloy should also consist β-Al<sub>3</sub>Mg<sub>2</sub> precipitates. A confirmation of this thesis is presented in Fig. 8a. The β phase precipitates of size ~150 nm are plate like morphology. In Fig. 8b and c, there is presented diffraction pattern and the solution that confirms the presence of Al<sub>3</sub>Mg<sub>2</sub> phase.

3.2. Mechanical properties

3.2.1. Hardness

In order to most beneficial heat treatment conditions of the investigated alloy a series of experiments was performed including diversified influence of solution treatment time and artificial ageing time. As it can be observed in Table 4

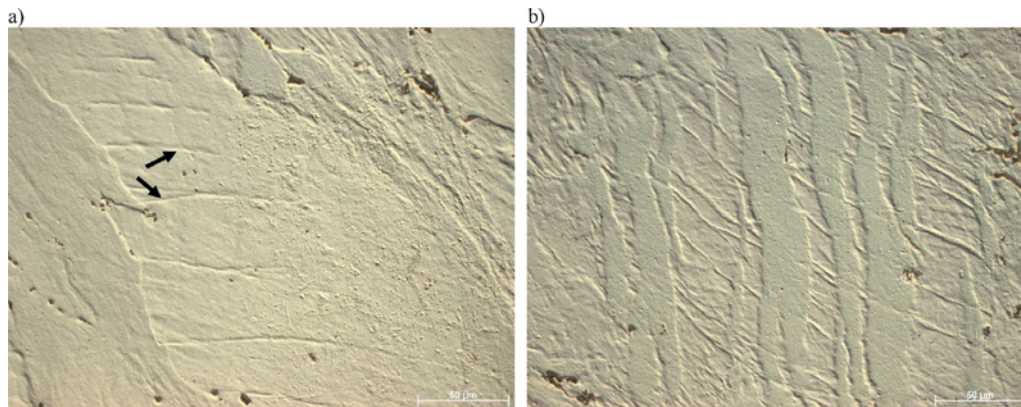


**Fig. 3 – Structure of AlMg3 alloy subjected to ECAP showing (a) slip bands in elongated grain, (b) shearing bands (mag. 500× C-DIC contrast).**

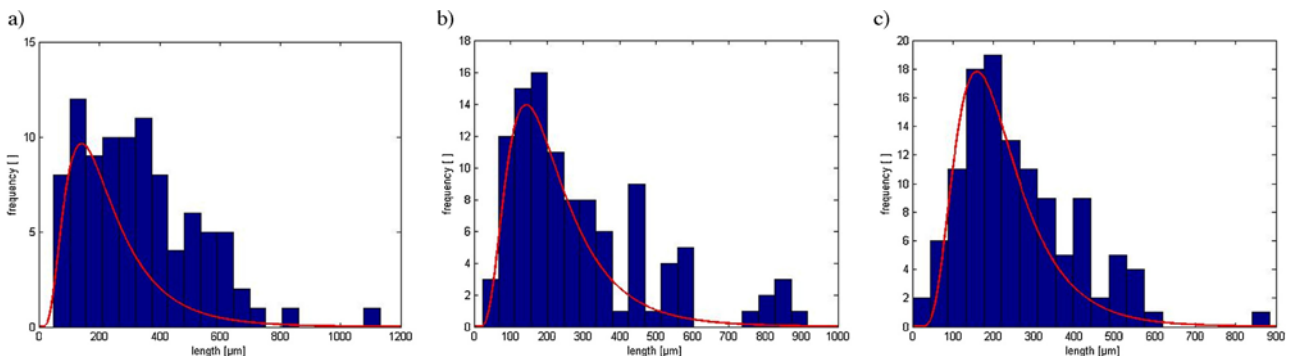


**Fig. 4 – Examples of histograms of grain distribution in AlMg3 alloy (a) initial state, (b) solution treated, (c) solution treated and ECAPed 4× route B<sub>c</sub>.**

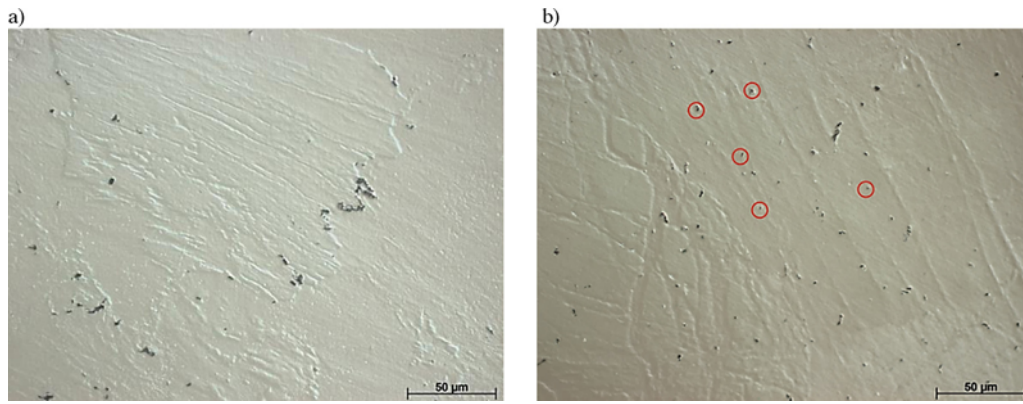


Fig. 5 - Microstructure of AlMg3 alloy (a) Solution treated and ECAPed, (b) Solution treated - ECAPed and aged at 160 °C 2 h (C-DIC contrast).

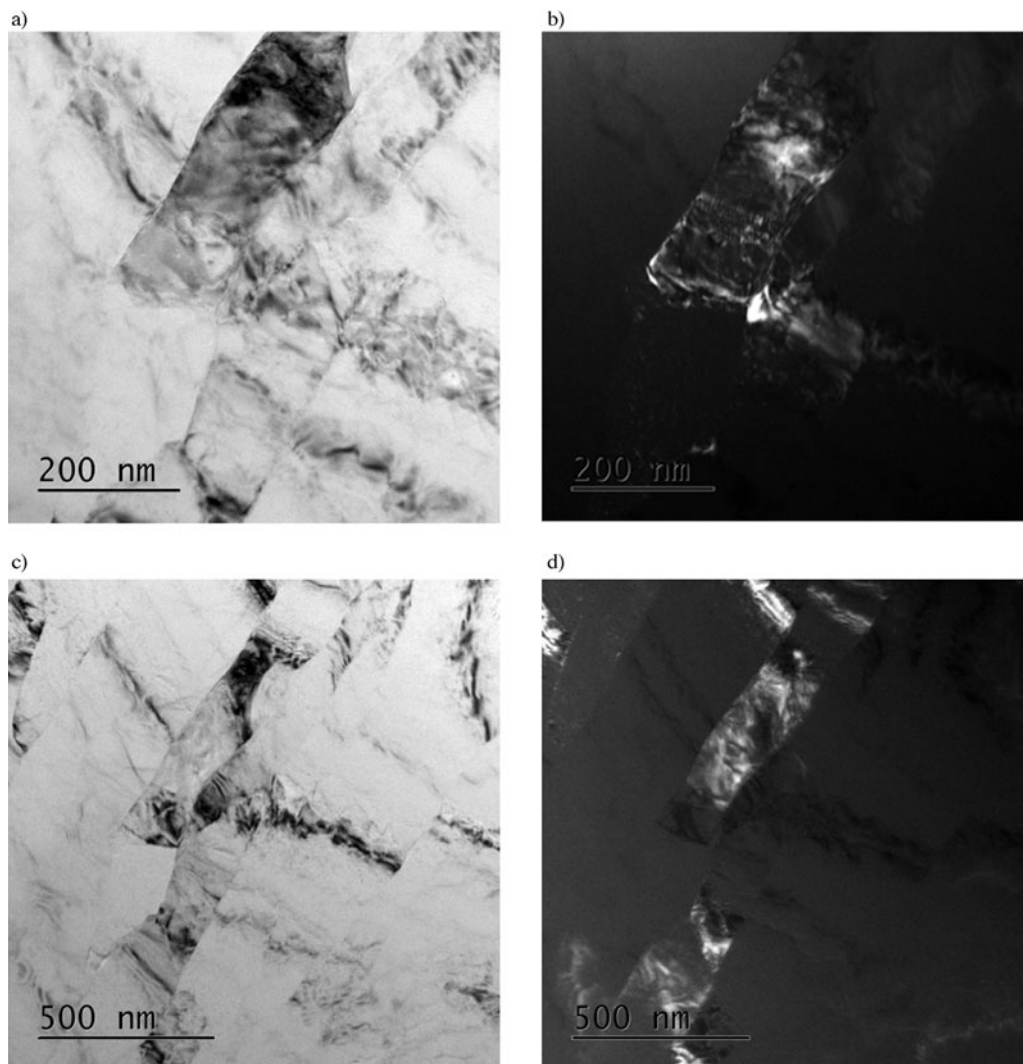


Fig. 6 - Representative TEM image of Solution treated-ECAPed and aged at 160 °C 2 h showing the elongated ultrafine grains of AlMg3 alloy, (a, c) bright field, (b, d) dark field.

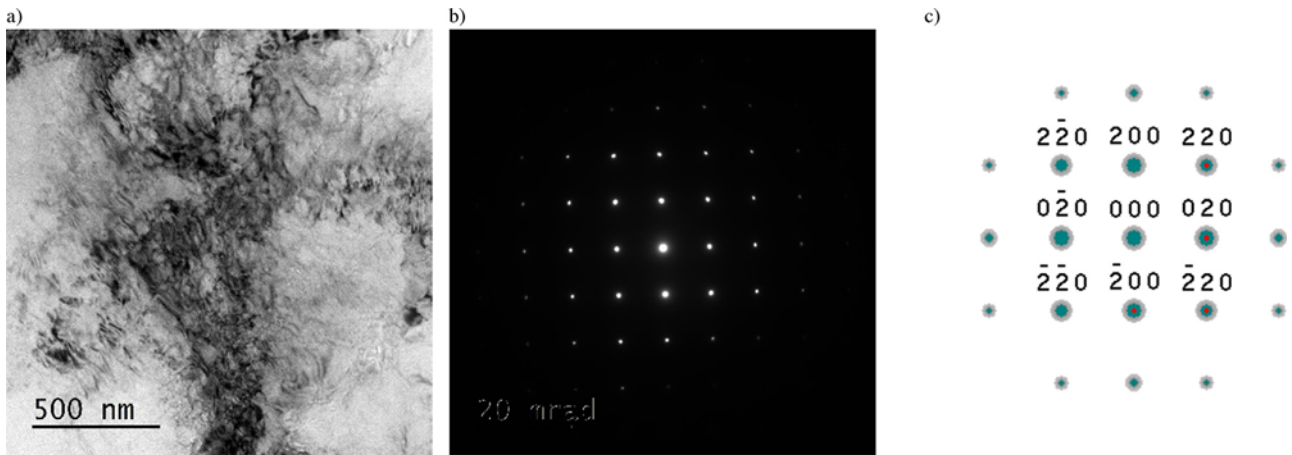


Fig. 7 – (a) Representative TEM image of solution treated – ECAPed and aged at 160 °C 2 h showing the high dislocation density area, (b) diffraction pattern, (c) solved diffraction pattern Al[001].

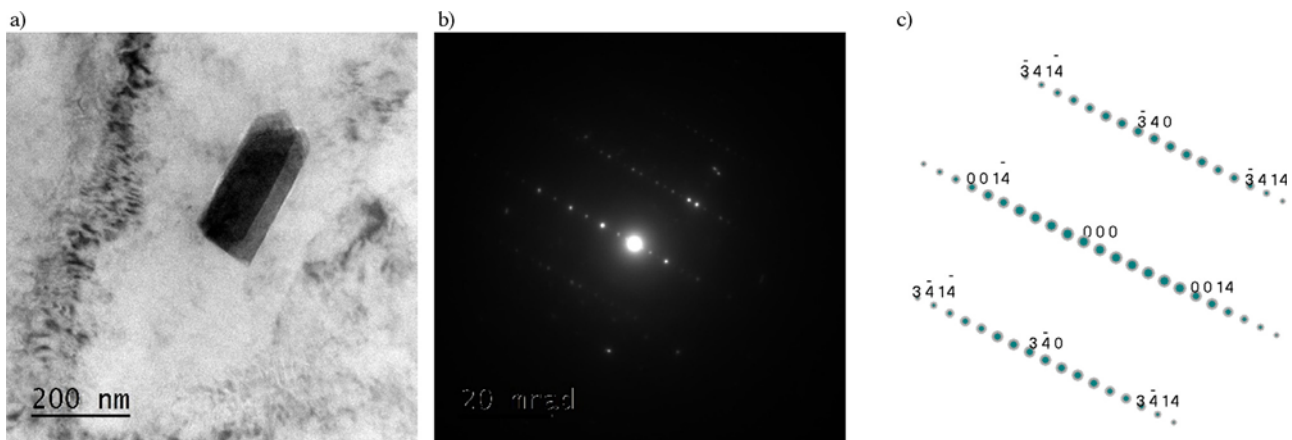


Fig. 8 – (a) Representative TEM image of Solution treated – ECAPed and aged at 160 °C 2 h showing the β-Al<sub>3</sub>Mg<sub>2</sub> precipitate, (b) diffraction pattern, (c) solved diffraction pattern Al<sub>3</sub>Mg<sub>2</sub>[-4-30].

examined alloy exhibits ageing potential and there is large increase in hardness even after 4 h of ageing therefore in further investigation this conditions were chosen.

Fig. 9 presents variation of  $H_V$  microhardness in function of ageing time at temperatures 100 °C and 160 °C of solution treated alloy before equal channel angular pressing and severely deformed without solution treatment. A significant increase in hardness occurs after four presses respect to the initial state 47  $H_V$  up to about 104  $H_V$ . This large increase in hardness can be connected with appreciable subgrain refinement and increased density of defects in the structure caused by severe plastic deformation [5]. Even in case of samples without heat treatment there is small increase in hardness after 2 h of artificial ageing visible comparing to as extruded state. Further artificial ageing results in decrease in hardness after 4 h which could be related to recrystallization or recovery process after low temperature annealing which is artificial ageing. Different effect is observable when samples were solution treated before severe plastic deformation. When supersaturated solid solution is subjected to artificial ageing

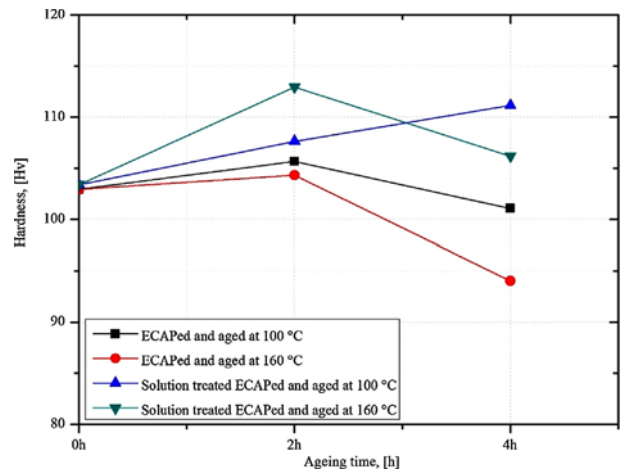
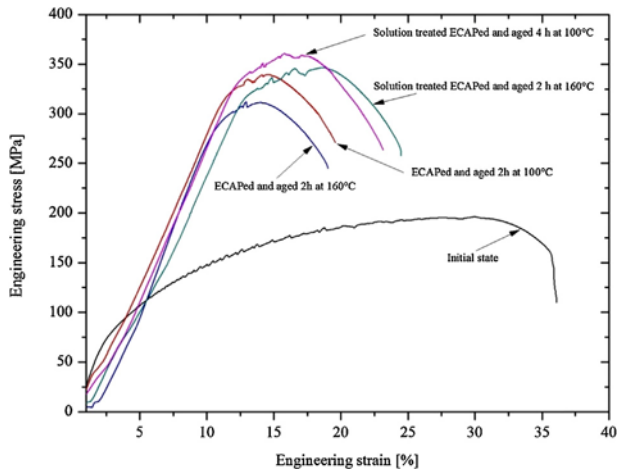


Fig. 9 – Variations of Vickers hardness of ECAPed AlMg3 alloy in function of ageing time.



**Fig. 10 – Engineering stress–strain curves of examined samples.**

increase in hardness is observed. When ageing is performed at higher temperatures peak appears after 2 h of ageing at 160 °C at value of hardness 113  $H_v$  which means that there is 10% increase in hardness compared to as pressed material. Even low temperature ageing causes increase in hardness but the peak is delayed and increase could be observed after 4 h where the value of hardness is 111 (about 9% more than after extrusion). This phenomena allows to conclude that formation of  $\beta'$  hardening precipitates in early stages of artificial ageing process outperforms the influence of dislocations recovery on the properties. However further ageing at 160 °C results in microhardness decrease which could be related to supremacy of dislocation density reduction through recovery process and depletion of the solutes in solid solution. The increase in hardness at 100 °C could be explained by the same phenomena but ageing at lower temperatures causes delay in formation of  $\beta'$  precipitates which results in observable increase in hardness after 4 h. Similar ageing phenomena has been reported in large group of aluminium alloys usually containing Cu or Si [16,18].

**3.2.2. Tensile behaviour at room temperature**

Tensile properties were obtained for the initial state alloy, after ECAP process and different post ECAP treatments. Two samples from non heat treated ECAPed and solution treated ECAPed that has highest hardness (Fig. 8) after artificial ageing were selected to tensile test. Unfortunately, each ECAPed sample only provide material to prepare specimen for one single test, thus the results could be not precise but even this

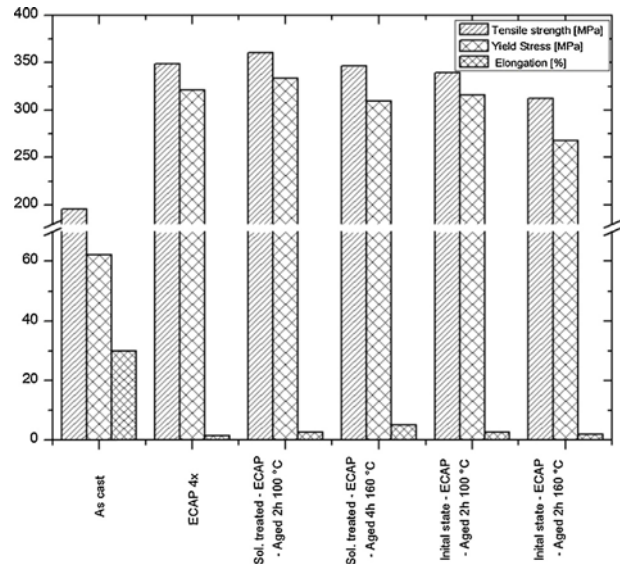


**Fig. 11 – Mechanical properties of investigated alloy after different treatments.**

fact the tendency is clear and it was found that much improvement in strength was achieved for all ECAP processed samples. The engineering stress-strain curves of initial state alloy and selected samples after ECAP with post-ageing treatment are shown in Fig. 10 Mechanical properties of initial state alloy compared to selected samples after ECAP with post-ageing treatment are shown in Fig. 11. As it could be observed there is significant increase in material subjected to severe plastic deformation even without heat treatment before ageing. The yield strength is highest for specimen solution treated before ECAP and aged for 4 h at 100 °C and is higher by 84% than that in initial state (~190 MPa) and higher than after extrusion (~12 MPa). Comparable values of yield strength was obtained for alloy after solution treatment before ECAP and artificial aged for 2 h at 160 °C. There also could be seen that the elongation is higher in comparison to previous specimen, which means that this method of treatment provides to obtaining more ductile material without significant decrease of tensile strength. Ageing at lower temperatures leads to decrease in mechanical properties without observable increase in ductility of material.

**3.2.3. Wear resistance**

Results of width of wear profile measurements and the friction coefficient are listed in Table 5. Because of small size of specimen used to tribological tests, measurement of wear field

**Table 4 – Results of hardness measurement of AlMg3 alloy in as cast state and after heat treatment.**

Temperature (°C)	Solution treatment time (h)	Hardness (as cast) $H_{V0.3}$	Hardness (solution treated) $H_{V0.3}$	Hardness (ageing 160 °C) $H_{V0.3}$		
				4 h	8 h	12 h
580	8	47.5	50.5	62.6	65.2	66.4
	12		51.2	61.6	63.9	64.1

**Table 5 – Results of width of wear profile measurements.**

	ECAPed 4× B <sub>c</sub>	Solutionized ECAPed 4× aged at 100 °C 2 h	Solutionized ECAPed 4× aged at 100 °C 4 h	Solutionized ECAPed 4× aged at 160 °C 2 h	Solutionized ECAPed 4× aged at 160 °C 4 h
Width of wear profile (μm)	2626	2585	2338	2538	2252
Friction coefficient	0.318	0.085	0.086	0.083	0.084

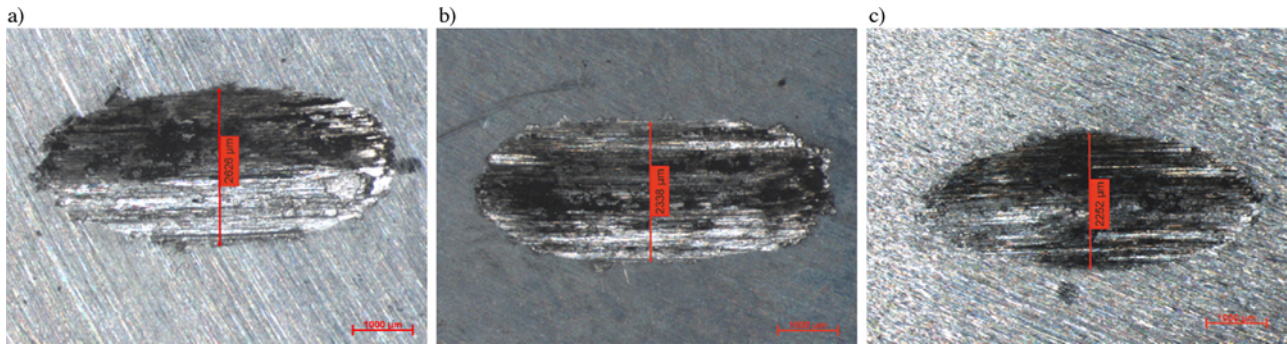


**Fig. 12 – Stereoscopic image of wear surface profile of: (a) Solutionized ECAPed 4× route B<sub>c</sub>, (b) Solutionized ECAPed 4× route B<sub>c</sub> aged 4 h 100 °C, (c) solutionized ECAPed 4× route B<sub>c</sub> aged 4 h 160 °C.**

was not possible, however higher wear resistance could be related with decreased width of wear profile. As it can be observed the width of tribological wear and the friction coefficient (Fig. 12a–c) is highest for the sample that was subjected to ECAP process without subsequent ageing process. Ageing process of as ECAPed specimens have a significant influence on the tribological properties of material. Comparison with hardness measurement results that are given in Fig. 9

and Table 4 allows conclusion that the ageing of ECAPed material increases not only hardness but also tribological properties of material. Width of wear profile for sample without ageing treatment is about 2626 μm. After ageing at 100 °C there could be observed that after 2 h of precipitation treatment width of wear profile decreases to 2585 μm with simultaneously small increase in hardness. When the hardness is highest (specimen aged for 4 h) width of wear profile

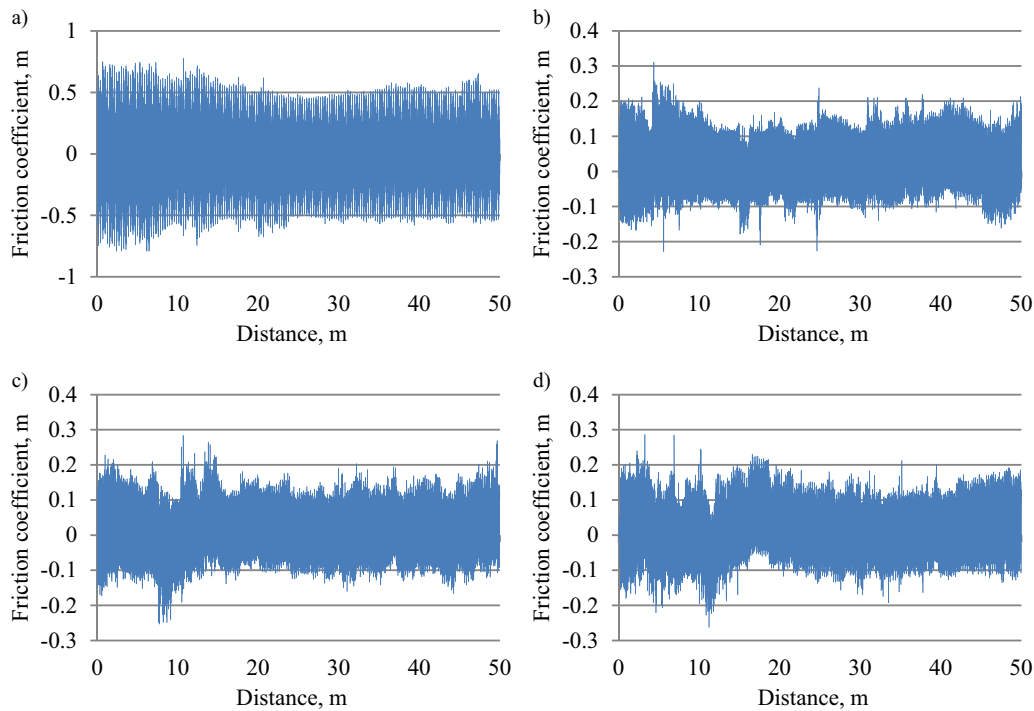


**Fig. 13 – Results of friction coefficient measurement in function of a distance (a) as ECAPed state, (b) solutionized ECAPed 4× route B<sub>c</sub> aged 2 h 160 °C, (c) solutionized ECAPed 4× route B<sub>c</sub> aged 4 h 160 °C, (d) solutionized ECAPed 4× route B<sub>c</sub> aged 4 h 100 °C.**



**Table 6 – Results of residual stress measurements.**

State	Residual stress (MPa)
Solution treated – ECAPed	49.6 ± 1.8
Solution treated – ECAPed aged at 100 °C 4 h	18.7 ± 1.9
Solution treated – ECAPed aged at 160 °C 2 h	3.8 ± 2.4

decreases to 2338  $\mu\text{m}$ . Similar fact could be observed for samples that were aged at 160 °C but after 4 h of ageing when the hardness starts to decrease the opposite fact may be observed (lower hardness results lowest wear profile). It could be connected with greater amount of the  $\beta''$  precipitates that forms during ageing process and increase the wear properties of material even when hardness starts to decrease. The change of friction coefficient in function of sliding distance in specimen subjected to ageing process (Fig. 13a–d) allows judging that the differences of friction coefficient could be caused by the re-bonding of big second phase precipitations which can be explained by the detachment of big second phase particles or the micro machining effect.

### 3.3. XRD residual stress measurement

As it was shown earlier structural changes that proceed in early stages of recovery process are hard to observe using ordinary metallographic techniques. However evidence of structural changes are possible to identify using X-ray diffraction techniques. As it was described by Hatch et al. [7] during recovery process in cold worked aluminium alloys dislocations are rearranged into cellular subgrain structure which process is often called polygonization. With increasing time and temperature of the process polygonization process is more rapid which results in an increase of subgrain size. At this stage many subgrains have grain boundaries that are completely free of dislocation. Reduction of dislocation density is caused by the effect of annealing and results in decrease of strength. Recovery that is induced by annealing may also results in changes in other properties of cold worked aluminium such as the increase in electrical conductivity, X-ray line broadening and reduction in residual stresses, thus XRD measurements method is quite good in characterization of structural changes that proceed during that process.

According to the geometry of the as pressed sample high residual stresses are expected perpendicular to the extrusion direction. The presented diffraction measurements are focussed on this region. It is worth to note that  $\sin^2 \psi$  method has the advantage to measure residual stresses independent of any changes in the stress free lattice spacing. X-ray diffraction measurements were performed in order to determine the average lattice strain in alloy subjected to ECAP after different post-ECAP treatments and are compared to the as pressed sample solution treated before deformation. Stress measurements results are given in Table 6. As it could be seen lattice strain are highest about 50 MPa for sample after ECAP and further ageing results in decrease of strain. After 2 h of artificial ageing at 160 °C residual stresses starts to disappear which could be subjected to recovery process. Lower ageing temperatures also provides to decrease in lattice strain but do not

remove them completely. Lattice strain measurements could be compared with tensile properties presented in Fig. 10. Specimen after ageing at lower temperature has higher tensile strength but the elongation is lower than in specimen after ageing at 160 °C. It could be concluded that recrystallization or recovery process proceed faster when artificial ageing is carried out at higher temperatures and removes almost completely microstrains in as pressed material.

## 4. Conclusions

Structure investigations demonstrate that ECAP process connected with post ageing treatments allows obtaining highly deformed grains that contains high density of shearing bands. Results of grain size measurement confirms that after solution treatment there is small decrease in grain size (increased amount of small grains). Further ECAP process also causes subsequent grain refinement. Observations of microstructure after ageing process using light microscopy do not allow observing any changes in microstructure.

The TEM analysis shows that there are presented in the structure of the severely deformed alloy two different areas, those defects free and with high dislocation density. It was also confirmed the presence of main hardening phase that occurs after artificial ageing. It was also found that the grain refinement occurs on the subgrain level.

Equal channel angular pressing has a meaningful influence on mechanical properties and increase hardness about 76% in comparison to as cast material. Further post ECAP ageing treatments also slightly increase hardness and yield strength of ECAPed material according to precipitation treatment, but ageing at lower temperature 100 °C do not increase ductility. Ageing of material subjected to equal channel angular pressing without heat treatment conducted before, provides to decrease in material properties which means that as cast material do not exhibit ageing potential and the diminishing of hardness is caused by a string recovery process. The results of wear resistance measurements also confirms that subsequent artificial ageing after ECAP process in samples that were solution treated increase wear properties of material. Greatest wear properties were observed for samples that were aged 4 h which can be connected with increased amount of secondary precipitates that appear during precipitation treatment in investigated aluminium alloy.

The results of X-ray diffraction lattice strain measurements confirm the presence of tension microstrains. There was also observed that during post ECAP heat treatment in higher temperatures the lattice strains starts to disappear which could correspond to recovery process that proceed during ageing.

## Acknowledgements

This paper has been elaborated in the framework of the project “Support research and development in the Moravian-Silesian Region 2013 DT 1 – International research teams” (02613/2013/RRC) – financed from the budget of the Moravian-Silesian

Region Czech Republic on the base of co-operation with VŠB – Technical University of Ostrava, Faculty of Mechanical Engineering.

## REFERENCES

- [1] R. Haghayeghi, P. Kapranos, An investigation on work hardening of Al-1%MG processed by Equal Channel Angular Pressing, *Materials Letters* 129 (2014) 182–184.
- [2] V.M. Segal, Engineering and commercialization of equal channel angular extrusion (ECAE), *Materials Science and Engineering A* 386 (1–2) (2004) 269–276.
- [3] T. Tański, A.D. Dobrzańska-Danikiewicz, K. Labisz, W. Matysiak, Long-term development perspectives of selected groups of engineering materials used in the automotive industry, *Archives of Metallurgy and Materials* 59 (4) (2014) 1717–1728.
- [4] R.Z. Valiev, R.K. Islamgaliev, I.V. Alexandrov, Bulk nanostructured materials from severe plastic deformation, *Progress in Materials Science* 45 (2) (2000) 103–189.
- [5] L. Man-ping, S. Shao-chun, H.J. Roven, Y. Ying-da, Z. Zhen, M. Murashkin, R.Z. Valiev, Deformation defects and electron irradiation effect in nanostructured AlMg alloy processed by severe plastic deformation, *Transactions of Nonferrous Metals Society of China* 22 (2012) 18101816.
- [6] L.A. Dobrzański, W. Borek, Hot-rolling of advanced high-manganese C-Mn-Si-Al steels, *Materials Science Forum* 706–709 (2012) 2053–2058.
- [7] J.E. Hatch (Ed.), *Aluminium Properties and Physical Metallurgy*, American Society for Metals, 2005 116–118.
- [8] M.H. Goodarzy, H. Arabi, M.A. Boutorabi, S.H. Seyedein, S.H. Hasani Najafabadi, The effects of room temperature ECAP and subsequent aging on mechanical properties of 2024 Al alloy, *Journal of Alloys and Compounds* 585 (2014) 753–759.
- [9] R.Z. Valiev, T.G. Langdon, Principles of equal-channel angular pressing as a processing tool for grain refinement, *Progress in Materials Science* 51 (7) (2006) 881–981.
- [10] M.H. Shaeri, M.T. Salehi, S.H. Seyyedein, M.R. Abutalebi, J.K. Park, Microstructure and mechanical properties of Al-7075 alloy processed by equal channel angular pressing combined with aging treatment, *Materials & Design* 57 (2014) 250–257.
- [11] W.J. Kim, C.S. Chung, D.S. Ma, S.I. Hong, H.K. Kim, Optimization of strength and ductility of 2024 Al by equal channel angular pressing (ECAP) and post-ECAP aging, *Scripta Materialia* 49 (4) (2003) 333–338.
- [12] T. Tański, K. Labisz, B. Krupińska, M. Krupiński, M. Król, R. Maniara, W. Borek, Analysis of crystallization kinetics of cast aluminum-silicon alloy, *Journal of Thermal Analysis and Calorimetry* (2015), <http://dx.doi.org/10.1007/s10973-015-4871-y>.
- [13] B. Tomiczek, M. Kujawa, G. Matula, M. Kremzer, T. Tański, L. A. Dobrzański, Aluminium AlSi12 alloy matrix composites reinforced by mullite porous preforms, *Materialwissenschaft und Werkstofftechnik/Materials Science and Engineering Technology* 46 (4) (2015) 368–376.
- [14] L.A. Dobrzański, W. Borek, Thermo-mechanical treatment of Fe-Mn-(Al, Si) TRIP/TWIP steels, *Archives of Civil and Mechanical Engineering* 12 (3) (2012) 299–304.
- [15] J. Wang, M. Furukawa, Z. Horita, M. Nemoto, R.Z. Valiev, T.G. Langdon, Enhanced grain growth in an Al–Mg alloy with ultrafine grain size, *Materials Science and Engineering A* 216 (October (1–2)) (1996) 41–46.
- [16] M. Vaseghi, H.S. Kim, A combination of severe plastic deformation and ageing phenomena in Al–Mg–Si Alloys, *Materials & Design* 36 (2012) 735–740.
- [17] S. Dadbakhsh, A. Karimi Taheri, C.W. Smith, Strengthening study on 6082 Al alloy after combination of aging treatment and ECAP process, *Materials Science and Engineering A* 527 (18–19) (2010) 4758–4766.
- [18] E.F. Prados, V.L. Sordi, M. Ferrante, The effect of Al<sub>2</sub>Cu precipitates on the microstructural evolution, tensile strength, ductility and work-hardening behaviour of a Al–4 wt.% Cu alloy processed by equal-channel angular pressing, *Acta Materialia* 61 (1) (2013) 115–125.
- [19] M. Baig, E. El-Danaf, J. Mohammad, Thermo-mechanical responses of an aluminium alloy processed by equal channel angular pressing, *Materials & Design* 57 (2014) 510–519.
- [20] M.J. Starink, A.-M. Zahra,  $\beta'$  and  $\beta$  precipitation in an Al–Mg alloy studied by DSC and TEM, *Acta Materialia* 46 (10) (1998) 3381–3397.
- [21] S. Rusz, L. Cizek, M. Salajka, S. Tylsar, J. Kedron, V. Michenka, T. Donic, E. Hadasik, M. Klos, Ultrafine grain refinement of AlMn1Cu and AZ 31 alloys by SPD process, *Archives of Metallurgy and Materials* 59 (1) (2014) 357–362. , <http://dx.doi.org/10.2478/amm-2014-0060>.